The International Journal of Advanced Manufacturing Technology (2018) 96:3311–3319
https://doi.org/10.1007/s00170-018-1837-9

ORIGINAL ARTICLE

Effects of the relative tool rotation direction on formability during the incremental forming of titanium sheets

E. H. Uheida[1] · G. A. Oosthuizen[1] · D. M. Dimitrov[1] · M. B. Bezuidenhout[1] · P. A. Hugo[1]

Received: 22 September 2017 / Accepted: 25 February 2018 / Published online: 3 March 2018

Abstract
The effects of tool rotation direction during single point incremental forming of pure titanium were experimentally studied. Axisymmetric components with a varying wall angle were formed using a round-tipped tool of 10 mm diameter and following a 3D spiral tool path. Test runs were executed by changing one factor at a time. Spindle rotation was tested in both the climb and the conventional directions. Tool step depth between runs was increased by a fixed interval over the range of 0.35 mm up to the plate thickness of 0.8 mm. The experimental results obtained by a comparison between the two forming strategies and their impact on the characteristics of formability are discussed in this paper. The achieved level of the forming angle (75°), and the reduction in geometric deviations from the conventional strategy, presents interesting findings. Considerable variations in the trends of forces and temperature between the two forming strategies are presented and discussed.

Keywords Comparison analysis · Relative velocity · SPIF · Thermomechanical effect · Titanium

1 Introduction

Single point incremental forming (SPIF) is an evolving flexible manufacturing process, where a sheet is formed into a final shape by a series of small incremental deformations. The process allows the production of geometrically complex sheet components, while requiring less tooling, and standard CNC equipment. In addition to the setup simplicity, the higher forming limits and lower forming forces as compared to conventional pressing are an attractive and promising aspect. Being characterised by long processing time, SPIF is typically suited for fabricating of customised parts, small series, or for rapid prototyping of thin-walled components.

Because of a lack of sheet support, SPIF is characterised by relatively low geometrical precision, when compared to conventional sheet forming techniques. This has resulted in few industrial applications of the process. To improve forming accuracy by reducing material springback, several measures have been suggested in literature. Allwood et al. [1] studied forming of both simple and complex components of sheets, which have been partially cut out into various designs of slots and tabs. They found that the cut out had very little effect on accuracy, in comparison to rigid backing support method. On the contrary, Otsu et al. [2] tested enhancing blank bending stiffness using embossed sheets, and found that the deviations at both the sample flange and the formed depth were decreased. Zha et al. [3] proposed forming technique based on fastened pre-tensioning, to produce a medical prosthesis from aluminium (1060H24) sheets. The pre-tensioning stresses reduced material springback; however, it created inhomogeneous distribution of the sample thickness due the frictional stress. Panjwani et al. [4] deliberated a flexible multipoint-die, which comprises an array of adjustable bolts to support workpiece backside. The reconfigurable setup allows for forming of complex and asymmetric components with reduced geometrical deviations.

Significant research has been conducted on optimising forming trajectories to reduce geometric deviations in SPIF. For instance, Lu et al. [5] demonstrated the advantages of using feature-based tool paths in forming different geometries, as compared to conventional z-height-based slicing algorithms. They reported that the forming accuracy and surface quality of the components are improved and forming time is reduced. Fiorentino et al. [6] presented a correction algorithm of the tool path, based on the iterative learning control technique, in relation with the actual part shape and the error distribution.

✉ E. H. Uheida
uheida@sun.ac.za; emadoheda@gmail.com

[1] Stellenbosch Technology Centre, Department of Industrial Engineering, Stellenbosch University, Stellenbosch, South Africa

Allwood et al. [7] underlined the importance of closed-loop control of properties in metal forming to compensate for the uncertainty. The article refers to the challenges in implementation of this topic, particularly for flexible (SPIF) processes, due to the unpredictability of the process mechanics. A framework for analysis, both temporal and spatial dynamics, in metal-forming control systems is also proposed. McAnulty et al. [8] conducted a quantitative review on a collection of highly relevant articles, which have studied the effect of SPIF parameters on formability. The paper underlined the universal parameters necessary to control the process. Collective data on the operating range of these parameters have also been presented.

Curiously, very few publications consider the effect of the direction of tool rotation on the forming process. The aspect of rotation direction seems insignificant. There is a paucity of literature on this issue:

> In their work, Otsu et al. [9] tested the effect of the rotation direction on the formability of aluminium A5052-H34 sheets. Two forming strategies similar to climb and conventional milling were tested. Results from their experiments show that similar levels of formability were achieved in both strategies. Slight improvements in the range of formable working conditions, as well as in accuracy, were associated with the conventional strategy.
>
> Durante et al. [10] studied the effect of tool rotational speed and direction, on the SPIF of aluminium AA 7075-T0 sheets. Despite the low level of speed (200–600 rpm) that was tested, a slight reduction in the horizontal force was reported, when switching the rotation from conventional to climbing. An increase in the forming temperature (by about 20%) when the tool was rotated against its feed direction, was also observed.
>
> Obikawa et al. [11] searched the influence of rotation direction under micro-forming conditions. They used two thicknesses of thin aluminium foil (50 μm and 12 μm), small tooltip radii (0.1 mm and 0.5 mm), and a desktop milling machine. The effect of an expanded range of tool rotations (-25,000 to +25,000 rpm) was examined. They reported that the rotating direction did not influence the forming limits.

The above-mentioned examples constitute all readily accessible publications. This underlines the lack of comprehensive information on the effect of the direction of tool rotation in the SPIF, and in particular for CP titanium sheets. This paper experimentally investigates this factor, while considering reasonable settings for the process variables. These settings have been established within a broader study directed towards mapping the SPIF process for CP titanium sheets [12]. In the sections following, a brief description of the test setup and a discussion of the observations are presented.

2 Experimental setup and design

A summary of the experimental setup and process settings that have been used in this study is given in this section, further details on the setup, equipment and the benchmark is reported in [12]. Figure 1 depicts the custom developed clamping rig fixed to a Kistler 9255C dynamometer, and mounted on a CNC table. The fixture design allows the execution of four consecutive test runs for a single test setup, saving on material and setting-up time, when compared to doing four individual tests instead.

A hemispherical, 10-mm diameter forming tooltip, made from tool steel 2312 and heat treated using TUFFRIDE process, was used. All test specimens were annealed CP grade 2, in the form of 0.8-mm thick sheeting. The specimen sheet size was 190 mm × 190 mm, and they were fitted symmetrically over the four working spaces of the clamping rig. The experimental work was performed with a gantry type, 3-axis (DMU 65 FD monoBlock) CNC machine centre. During the experiments, a Raytek MX4 IR camera (pyrometer) was pointed at the workpiece surface to obtain the temperature gradient at the deformation area. To intensify the pyrometer readings, the undersides of the specimens were spray painted to enhance and unify the emissivity of the titanium specimens. Spraymate Engine Enamel black spray paint, which is heat-resistant up to 110 °C, was used to paint the specimens. The lubrication method comprised the application of a thin layer of the 98.5% pure, dry MoS2 powder by gently rubbing it into the workpiece surface. Thereafter, the entire working surface was covered with the powder to a thickness of about 10 mm.

An axisymmetric conical geometry with varying wall angle was designed for the evaluation. It has a maximum inner diameter of 56 mm and depth of 25 mm. The CAD model wall angle starts from $\theta_i = 30^{\circ}$ at the sample opening, which increases to 75° at the bottom of the cone. As suggested by Khalatbari et al. [13], the wall angle was designed to increase by a constant ratio in accordance with the component depth (h_i), and is given by Equation 1.

$$\theta_i = 30 + 1.8 \cdot h_i \tag{1}$$

A 3D, out-to-in, spiral tool path with a constant step depth was used. The tool path was automatically generated from the CAD model of the test benchmark. Commercial CAD/CAM packages from Delcam, PowerSHAPE and PowerMill were respectively used to generate the benchmark geometry and the tool path. In SPIF, material formability is commonly characterised by the maximum wall angle (θ_{max} : degrees), without sheet fracture. Because the forming tool path was generated according to the CAD model as given by Equation 1, θ_{max} can be found by measuring the maximum depth (h_{max}) formed before sheet fracture and using the same formula. During the experiments, the tool feed rate (f) was set as 625 mm/min. The tool rotational speed (ω) of 1940 rpm was

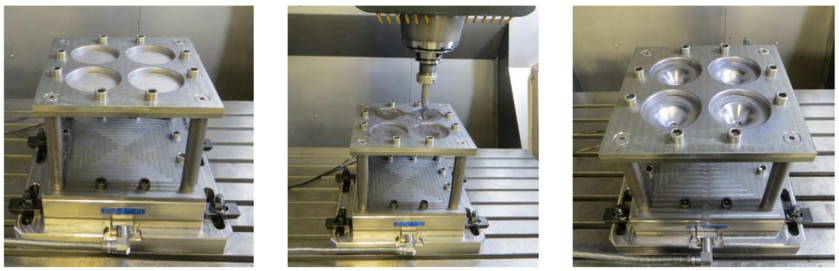

Fig. 1 Depiction of the test platform showing various stages of the forming process

fixed in the clockwise direction. Switching of the rotation direction from climbing to conventional was made by changing the tool path (feed) direction as illustrated in Fig. 2a.

The experiments were completed under increasing, dynamic load conditions. This was resulted from raising the tool step depth (Δz) by 0.15 mm between the test runs, starting with 0.35 mm and ending with 0.8 mm, which coincides with the samples thickness. In addition, the increase of the wall angle as the depth, h_i of the model being formed advances, enlarges the tool/sheet contact interface, which incrementally raises the forming forces required. This evolving wall angle of the model influences the relative velocity at the interface. As stated by Otsu et al. [9], the relative velocity can be identified for both rotation directions by Equation 2. For the climb direction, the feed rate is subtracted, reducing the relative velocity, while for the conventional direction, feed is added, making the relative velocity larger.

$$V = 2\pi \cdot \omega \cdot r \cdot sin\theta_i \pm f \tag{2}$$

The instant wall angle, θ_i of the geometry being formed, defines the effective contact radius ($r \cdot \sin\theta_i$) of the tooltip and accordingly changes V over different points of the interface. In Fig. 2b, the trends of relative velocity for the forming strategies have been determined by Equation 2 for the current process settings. As seen from the graph, V is proportional to the wall angle along the forming path. It is slightly higher by a constant value for the conventional direction, the value being twice the feed rate.

3 Discussion of the experimental results

The experimental results of the two groups of tests, based on direction of the tool rotation used, are set in a comparative form. If an obvious fracture was observed during the experiment, the test run had to be stopped. Otherwise, the test continued until the design depth of 25 mm was reached.

3.1 Evaluation of formability and surface quality of components

In Fig. 3, illustration of the inside and outside of the titanium components formed. It distinguishes between the two groups according to the direction of tool rotation applied. Due to overstretching of the sheet material, all the samples of group A cracked before reaching the designed depth.

As annotated on the outsides of the samples in Fig. 3a, the cracks occurred at few millimetres above the bottom, and parallel to the direction of tool feed. Formability in this group was not noticeably affected by the changes of step depth size. The maximum wall angle of the four samples remained at ($\theta_{max} = 65 \pm 1.4^{\circ}$) the typical level. Remarkably, for group B, the four samples were deformed to the desired geometry, without material failure. The forming angle for the four samples was estimated to be about 75°. This is a unique level of formability in so-called single-pass cold SPIF, when taking into consideration the 0.8-mm titanium sheet and the 10-mm tooltip used. As was established for group A, the effect of

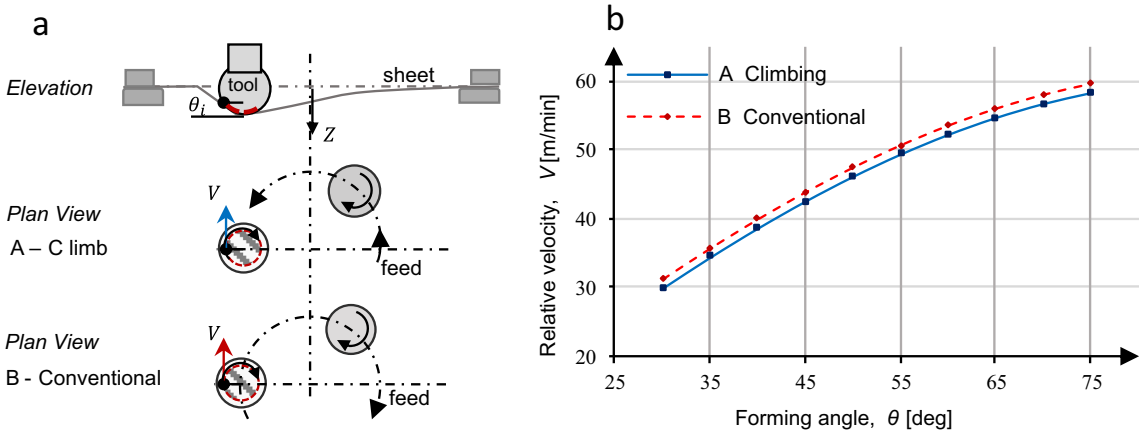

Fig. 2 The concept of climb and conventional forming. **a** Schematic of the forming tool paths. **b** Relative velocity versus the forming angle

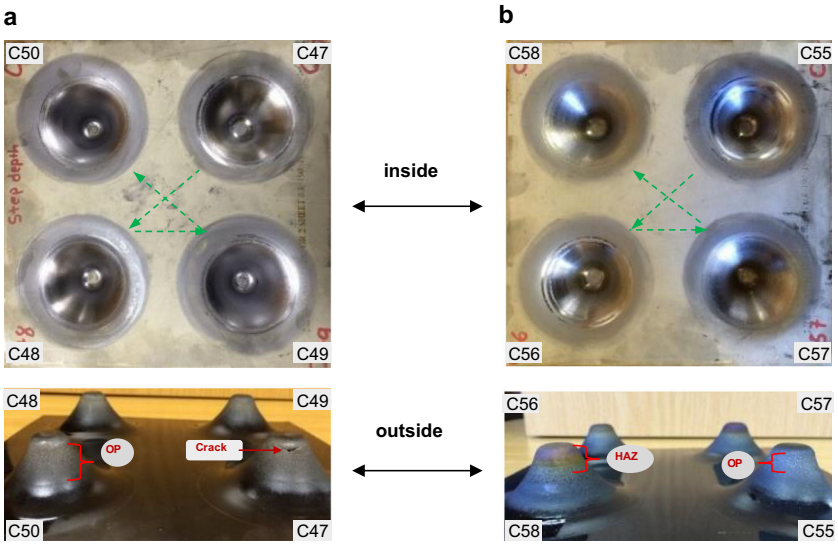

Fig. 3 Depiction of the components formed. **a** Climbing. **b** Conventional. Note inside and outside views are mirror images; the dashed arrows show the sequence of the runs and HAZ marks the heat-affected zone

the step depth size on the maximum wall angle for group B was also found to be negligible.

Although, surface roughness of the components was not quantitatively analysed, some qualitative assessment can however be conveyed. The initial samples from group A displayed a smooth and glossy surface on their inside. This finish progressively deteriorated slightly as the step depth, Δz was increased. On their outside surfaces, a roughening defect, known in sheet metal forming as orange-peel (OP), arose. The area affected by the OP was limited nearby the samples' bottoms. Severity of the OP defect visually increases between the samples proportional to the size of Δz used. The samples of group B showed relatively coarser surfaces on their insides. Signs of material peeling (milling action) occurred across the entire contact surface. This caused degradation of the surfaces, manifested by flaking of the titanium material. The burnout of these flakes produced flashes during the forming. The surface roughness intensified at larger Δz. On the outside of these samples (Fig. 3b), other than the OP effect, a heat-affected zone (HAZ) developed. The increased spread of both the OP and HAZ correlated directly with the increased size of step depth.

3.2 Evaluation of the geometric accuracy

The 2D contours of the inner surface of the samples were obtained using a coordinate measuring machine. The 3D geometries for the components were then regenerated with the aid of the PowerSHAPE package, by revolving the measured contours. This enabled the comparison of the experimentally obtained profiles to the ideal profile shape of the CAD model, by utilising the comparison analysis tool in the software. The two profiles are discretised into the same number of points, after which a point-to-point difference in coordinates is calculated and a deviation map fitted. Figure 4 shows the regenerated, cross-sectional profiles, coaxially plotted onto the designed profile geometry. The figure is accompanied by a summary of the maximum error values presented in Table 1. To examine the effect of Δz on the accuracy, the profiles from each group are arranged vertically, from smallest Δz, to the largest. The two groups are placed side-by-side to facilitate comparison of the effect of the rotation direction. For visual presentation and comparison purposes, the scale bar is fixed to the values of the overall maximum error, allowing for clear identification of difference in deviation between the various formed profiles.

Generally, in both the cases A and B, the profiles of the formed components are slightly smaller from the designed profiles. This is mainly due to elastic recovery of titanium sheeting occurred during and after forming. To compensate for elastic recovery of the sheet, small incremental deviations in keeping with the component size can be implemented overform. Shape deviations in the components were large in the proximity of the cone-opening flanges. These deviations are inevitable in the manufacture of SPIF components. This is related to sheet bending at this transition zone from global to local deformation. Once the sheet has undergone sufficient deformation so that it can locally support the tool force, the profile error falls away. Utilising of backing plate minimises the error due to sheet bending. The errors in the forming depth result from the bulging (concave upwards) of material caused by an accumulation of residual stresses. This effect is also known as pillow tendency, when it is intense, it can adversely affect accuracy and formability in SPIF. The effect can be minimised by extending the forming path across the bottom of the components [14, 15].

By comparing the accuracy for each group individually, following the vertical order of the plots, there was no regular trend on how Δz affected the accuracy. Although, geometrical deviations seem to vary (high/low) in a similar order for the

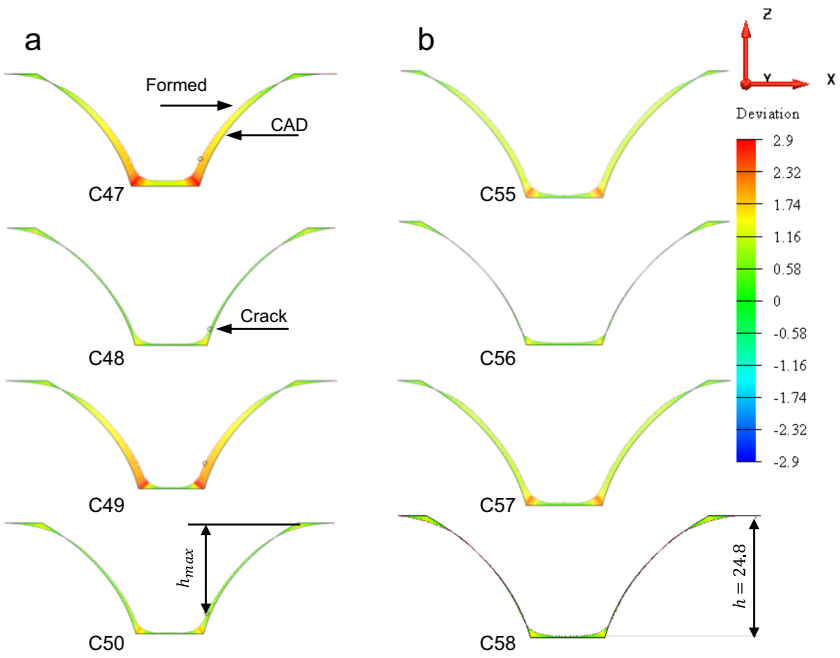

Fig. 4 Comparisons of cross-sectional profiles with the CAD model. **a** Climbing. **b** Conventional. Note that plots are arranged downward according their Δz size; the colours scale the deviations

two groups A and B, the variations appear to be unrelated to the size of Δz. The minimum deviation for both groups is found at a step depth of 0.5 mm (Table 1). More important is the reduction of the geometrical deviation of the samples of group B, when compared to their equivalents of A.

This section presented findings about the effect of tool rotation direction on formability and accuracy. In lieu of the sparsity of available literature, this seemingly insignificant factor does in fact yield a noticeable effect within the forming process. The following sections assess the effect on forces and temperatures generated in order to provide more insight into the thermomechanical behaviour associated to the two strategies.

3.3 Variations in the forming forces

In the SPIF process, there are mainly two types of forces involved: axial forces due to the helical step down of the tool path and horizontal (in-plane) forces resulting from the tool feed motion. These forces act simultaneously and continuously at the tool/sheet interface, as the tooltip, due to the embossed rotation, contacts and retracts from the interface [16]. A plot of the force gradients as measured during the experiments is shown in Fig. 5, and is supplemented with a summary on the maximum F_Z in Table 2. Due to the centrosymmetric profile of the samples formed, a plot of the in-plane forces F_X and F_Y are analogous to sine profiles. The profiles of these forces should be similar in (absolute value) magnitude and trend, but with a phase difference of $\pi/2$ between them. Hence, only the gradients of F_X are shown in the figure and will be discussed. The evolving of the axial force F_Z is, however, independent of the tooltip position on the x-y plane [17–19].

Comparing the trends of group A at different step sizes, both F_Z and F_X are directly influenced by the contact type, displaying a proportional dependence on the size of the step depth. Stepping Δz from 0.35 to 0.8 mm, there were corresponding increases of 35% in F_Z and 51% in F_X. By contrast for group B samples, a reduction by 51% in F_Z was observed when Δz was increased, while there were no noticeable changes in F_X, which remained almost the same over the four samples. The force gradients of group A reveal more steady and consistent trends than in the case of group B.

A closer look at the plots (Fig. 5b) of forces in B indicates an abnormal oscillation of the forces (waviness), which is evident in the F_X gradients along the forming path. The waviness can be coupled to the mill-like removal of material from the surface observed on the samples of this group. The

Table 1 The percentage change of the absolute shape deviations between the two groups

						Average
Step depth [mm]		0.35	0.50	0.65	0.80	
Max error [mm]	A	2.882	1.595	2.735	1.880	2.27
	B	2.270	1.454	2.243	1.472	1.86
Change of max error [%]		− 21	− 9	− 18	− 22	− 18

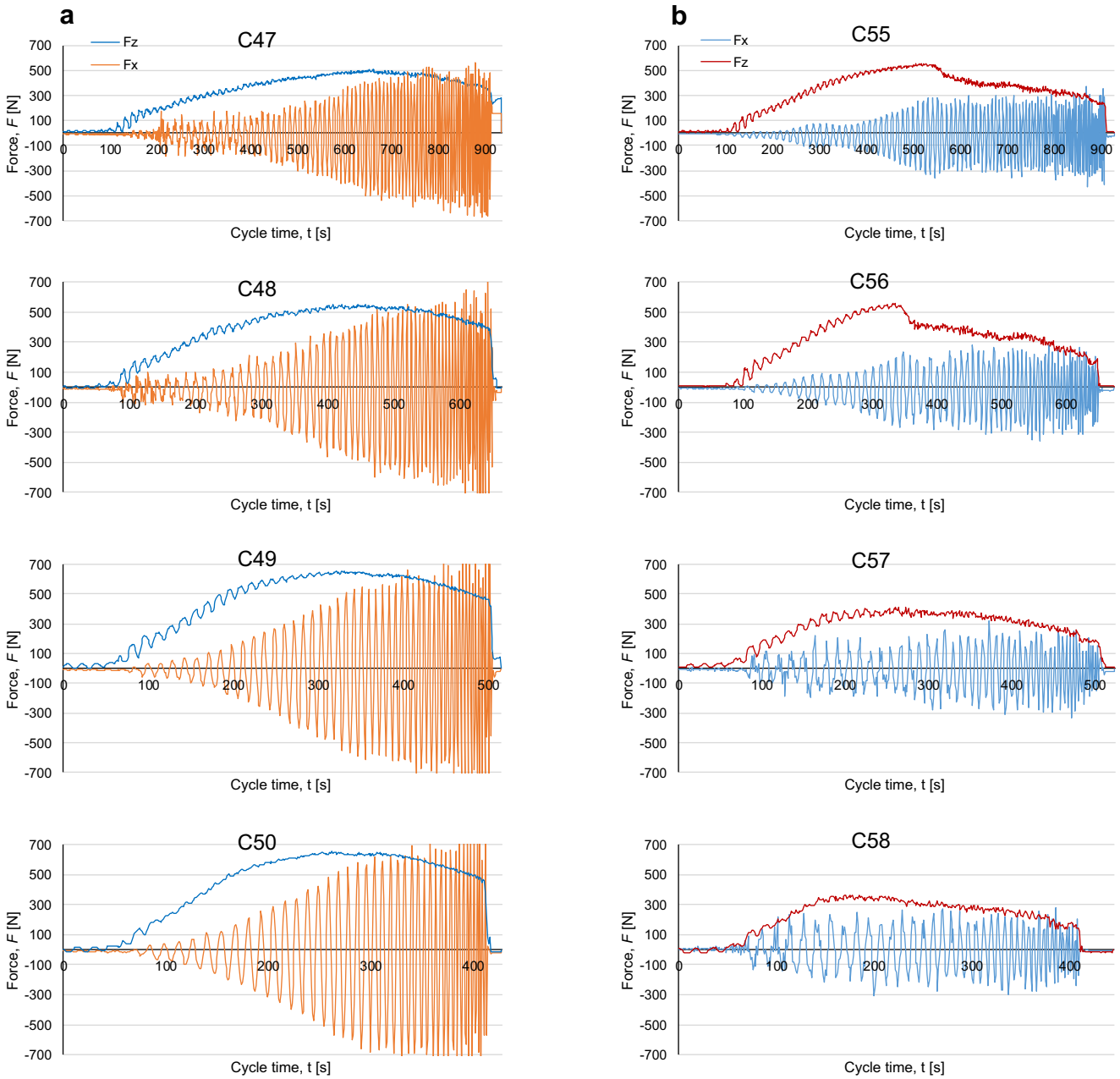

Fig. 5 Comparison of the gradients of forming forces at different step depth sizes. **a** Climbing. **b** Conventional

excessive friction and heat developed on group B samples led to degradation of the surface in the form of flaking of the titanium, as well as to escalated tool wear. The flaking and tool wear are the most probable cause of the irregular waviness of the force trends of group B. In group A, the rolling process results in the tooltip having a steadier revolving action over the surface, which reduces the sliding friction and produces a smoother trend in the change of forces.

Table 2 The change in the axial forces between the two groups

						Average
Step depth [mm]		0.35	0.50	0.65	0.80	
Max *Fz* [N]	A	444	475	589	601	527
	B	414	388	328	286	354
Change in the axial force [%]		− 7	− 18	− 44	− 52	− 33

Previously, the discussion has attempted to provide insight into the nature of formability and forces associated with deformation, but it is worth pointing out that this is intimately connected to the thermal cycle during the process. The next section discusses the forming temperature, which principally influences the nature of stresses, the material flow and elastic recovery.

3.4 Variations of the forming temperature

In SPIF, heat is generated due to friction between the tooltip and the workpiece, and some additional heat is produced by the adiabatic plastic working of the material. Figure 6 presents a graph of the instantaneous surface temperature measured during the forming of the samples, plotted against the cycle time. A summary of the maximum temperature readings is presented in Table 3.

The mean of the graphs shows a proportional relationship between the mean forming temperature and the size of Δz used. This was anticipated since tool/sheet contact and the amount of material to be formed at the interface increase, when Δz is stepped up. Improvement of process efficiency at a larger Δz can also be observed from the reduced cycle times, needed to accomplish the forming.

Noticeable in Fig. 6 are the higher mean temperatures related to the samples from group B (red dashed gradients) as compared to those of the blue curves for group A. The contrast between the gradients for each comparable pair of samples appears along the trajectory (cycle time). Table 3 shows the percentage of change in maximum forming temperatures (T_{max}) between A and B, which increases drastically for the samples formed with Δz above 0.5 mm. The improved formability and reduced deviations on the samples of group B can be correlated to the rise in temperature observed. The local dynamic heating has a pronounced effect on the thermal softening of titanium enhancing material ductility and reducing the forming forces required [20, 21]. It also minimised the deviations in the group B samples.

As demonstrated by Bhushan and Kennedy [22], the increase in the normal surface temperature, at the contact area, of two sliding bodies is a function of the amount of heat generated at the contact, the swept area, the coefficient of convection at boundaries, the frictional heat duration and a geometrical factor. Since all factors, except the frictional heating, can be considered comparable between group A and B, the only parameters that affect the increase in normal surface temperature are the amount of heat generated at the contact and the frictional heat duration. The frictional heating (q) between two sliding bodies is given by

$$q = \mu \cdot P \cdot V \tag{3}$$

Here, μ and P are, respectively, the coefficient of friction and the contact pressure, while V is the relative sliding velocity at the contact interface, as previously discussed. From Equation 2, V will vary in association with the process variables that determine the frictional and contact conditions at the interface. Accordingly, temperature trends varied along the forming path of each sample, and between runs of the same group, but with the largest variation between groups A and B. The relative directions of tool rotation (climbing/conventional) to the tool path direction evidently affected the relative velocity at the interface, which is higher in the advancing mode, and consequently affects the overall process outcomes. The combined diagram in Fig. 7 summarises the relationship between the above-discussed variations of the thermal and mechanical loads, in the two strategies, plot versus the step depth size.

The higher frictional heating observed in B was mostly concentrated along the swept surface, because of the low heat conductivity and poor rate of heat dissipation of titanium. The

Table 3 The change in the maximum temperature between the two groups

						Average
Step depth [mm]		0.35	0.50	0.65	0.80	
T_{max} [°C]	A	188	225	230	240	221
	B	235	264	342	355	299
Change in the T_{max} [%]		25	17	49	48	35

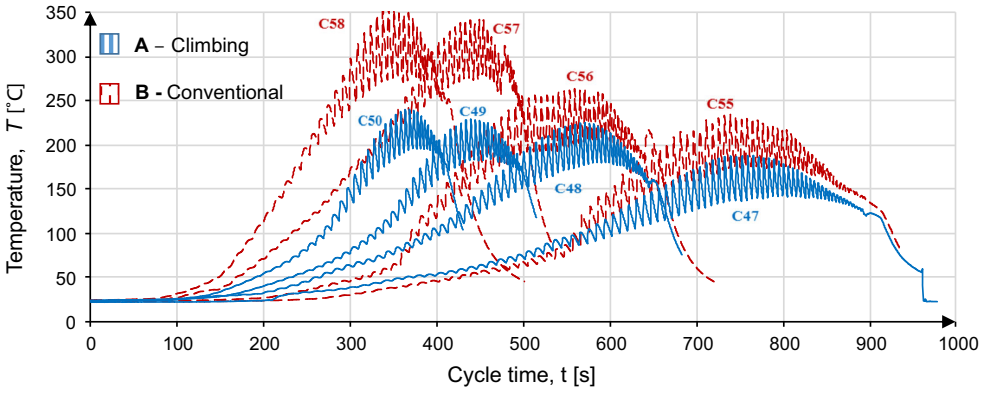

Fig. 6 Comparison of temperature gradients at different step depth sizes

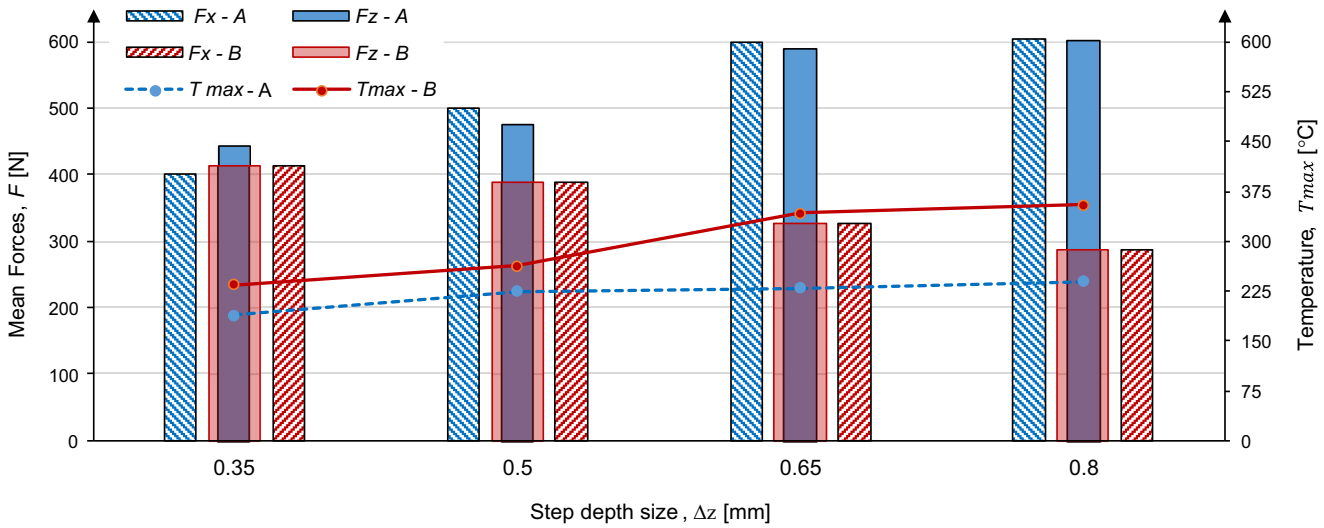

Fig. 7 All sets of the mean forces and maximum temperatures versus the step depth size

build-up heat activated thermal softening and ductility of the formed material. Consequently, low forming forces were required, and residual stresses and springback were relatively diminished.

4 Conclusions

This study was undertaken to evaluate effects of relative rotation directions of the tool to the tool path on formability, during SPIF of titanium. A sequence of experimental runs was performed in both the climb (A) and conventional (B) strategies, using samples of CP grade 2 sheets. Formability was evaluated by measuring the maximum wall angle produced. Forces and temperatures associated with the deformation process were also monitored and evaluated. The following main points can be concluded:

- In both strategies A and B, the forming temperature was proportional to the size of the step depth Δz; this is due to the enlarging deformation rate when Δz is raised.
- Forming forces (F_X, F_Z) in A were directly related to the increase in Δz. In B, the horizontal forces showed oscillating gradients, while axial forces dropped, when Δz is stepped up. The latter behaviour of the forces could be correlated to the significant rise in forming temperature (about 35%) observed in B, when Δz was increased.
- A 15% higher forming angle and fewer geometric deviations (better accuracy) were associated with the samples from group B, in comparison to those produced in A.
- Samples formed in B showed poor surface qualities and signs of overheated material due to excessive friction.

Although the study found evidence of variations of formability aspects between the two strategies, however, from the data collected, it was not possible to determine what effect due to rotation direction caused the variations. Future studies, including evaluation of stress gradients, during the two strategies, are therefore necessary to develop a better understanding of the processes affecting forming.

Acknowledgements The Stellenbosch Technology Centre staff members are acknowledged for their contribution to the experimental work.

Funding information The authors would like to thank the South African Department of Science and Technology for their financial support.

References

1. Allwood JM, Braun D, Music O (2010) The effect of partially cut-out blanks on geometric accuracy in incremental sheet forming. J Mater Process Technol 210:1501–1510. https://doi.org/10.1016/j.jmatprotec.2010.04.008
2. Otsu M, Uchimura T, Okada M, Yoshimura H, Matsumoto R, Muranaka T (2017) Friction stir incremental forming of preformed sheets with improving bending stiffness. Procedia Eng 183:131–136. https://doi.org/10.1016/j.proeng.2017.04.035
3. Zha GC, Shi XF, Zhao W, Gao L, Wu ML (2016) Experimental research of incremental sheet forming based on fastened pre-tensioning. Int J Adv Manuf Technol 82:711–717. https://doi.org/10.1007/s00170-015-7411-9
4. Panjwani D, Priyadarshi S, Jain PK, Samal MK, Roy JJ, Roy D, Tandon P (2017) A novel approach based on flexible supports for forming non-axisymmetric parts in SPISF. Int J Adv Manuf Technol 92:1–15. https://doi.org/10.1007/s00170-017-0223-3
5. Lu B, Chen J, Ou H, Cao J (2013) Feature-based tool path generation approach for incremental sheet forming process. J Mater

Process Technol 213:1221–1233. https://doi.org/10.1016/j.jmatprotec.2013.01.023
6. Fiorentino A, Giardini C, Ceretti E (2015) Application of artificial cognitive system to incremental sheet forming machine tools for part precision improvement. Precis Eng 39:167–172. https://doi.org/10.1016/j.precisioneng.2014.08.005
7. Allwood JMM, Duncan SRR, Cao J, Groche P, Hirt G, Kinsey B, Kuboki T, Liewald M, Sterzing A, Tekkaya AEE (2016) Closed-loop control of product properties in metal forming. CIRP Ann Manuf Technol 65:573–596. https://doi.org/10.1016/j.cirp.2016.06.002
8. McAnulty T, Jeswiet J, Doolan M (2016) Formability in single point incremental forming: a comparative analysis of the state of the art. CIRP J Manuf Sci Technol 16:43–54. https://doi.org/10.1016/j.cirpj.2016.07.003
9. Otsu M, Katayama Y, Muranaka T (2014) Effect of difference of tool rotation direction on forming limit in friction stir incremental forming. Key Eng Mater 622:390–397. https://doi.org/10.4028/www.scientific.net/KEM.622-623.390
10. Durante M, Formisano A, Langella A, Capece Minutolo FM (2009) The influence of tool rotation on an incremental forming process. J Mater Process Technol 209:4621–4626. https://doi.org/10.1016/j.jmatprotec.2008.11.028
11. Obikawa T, Satou S, Hakutani T (2009) Dieless incremental microforming of miniature shell objects of aluminum foils. Int J Mach Tools Manuf 49:906–915. https://doi.org/10.1016/j.ijmachtools.2009.07.001
12. Uheida EH (2016) Development and optimisation of incremental sheet forming of titanium grade 2: process mapping. Dissertation, University of Stellenbosch
13. Khalatbari H, Iqbal A, Shi X, Gao L, Hussain G, Hashemipour M (2015) High-speed incremental forming process: a trade-off between formability and time efficiency. Mater Manuf Process 30:1354–1363. https://doi.org/10.1080/10426914.2015.1037892
14. Essa K, Hartley P (2011) An assessment of various process strategies for improving precision in single point incremental forming. Int J Mater Form 4:401–412. https://doi.org/10.1007/s12289-010-1004-9
15. Al-Ghamdi K, Hussain G (2014) The pillowing tendency of materials in single-point incremental forming: experimental and finite element analyses. Proc Inst Mech Eng B J Eng Manuf 229:744–753. https://doi.org/10.1177/0954405414530906
16. Grimm TJ, Ragai I, Roth JT (2017) A novel modification to the incremental forming process, part 1: multi-directional tooling. Procedia Manuf 10:510–519. https://doi.org/10.1016/j.promfg.2017.07.035
17. Dakhli M, Boulila A, Tourki Z (2017) Effect of generatrix profile on single-point incremental forming parameters. Int J Adv Manuf Technol 93:1–12. https://doi.org/10.1007/s00170-017-0598-1
18. Xu D, Wu W, Malhotra R, Chen J, Lu B, Cao J (2013) Mechanism investigation for the influence of tool rotation and laser surface texturing (LST) on formability in single point incremental forming. Int J Mach Tools Manuf 73:37–46. https://doi.org/10.1016/j.ijmachtools.2013.06.007
19. Wang J, Nair M, Zhang Y (2017) An efficient force prediction strategy for single point incremental sheet forming. Int J Adv Manuf Technol 92:3931–3939. https://doi.org/10.1007/s00170-017-0422-y
20. Buffa G, Campanella D, Fratini L (2013) On the improvement of material formability in SPIF operation through tool stirring action. Int J Adv Manuf Technol 66:1343–1351. https://doi.org/10.1007/s00170-012-4412-9
21. Uheida E, Oosthuizen G, Dimitrov D (2017) Investigating the impact of tool velocity on the process conditions in incremental forming of titanium sheets. Procedia Manuf 7:345–350. https://doi.org/10.1016/j.promfg.2016.12.085
22. Bhushan B (2000) Frictional heating and contact temperatures. In: Mod. Tribol. Handb., illustrate. CRC Press, Columbus, pp 235–273